Geophysical Research Letters

RESEARCH LETTER
10.1029/2019GL084928

Sensitivity of Marine Heatwave Metrics to Ocean Model Resolution

Gabriela S. Pilo[1], Neil J. Holbrook[1], Andrew E. Kiss[2], and Andrew McC. Hogg[2]

[1]Institute for Marine and Antarctic Studies and Australian Research Council Centre of Excellence for Climate Extremes, University of Tasmania, Hobart, Tasmania, Australia, [2]Research School of Earth Sciences and Australian Research Council Centre of Excellence for Climate Extremes, Australian National University, Canberra, ACT, Australia

Key Points:
- Marine heatwaves are weaker, longer-lasting, and less frequent in models than in observations
- The higher the model resolution, the less biased the marine heatwave metrics
- Eddy-permitting models can be used for global marine heatwave analyses, but eddy-rich models are optimal for regional analyses

Correspondence to:
G. S. Pilo,
gabriela.semolinipilo@utas.edu.au

Citation:
Pilo, G. S., Holbrook, N. J., Kiss, A. E., & Hogg, A. M. (2019). Sensitivity of marine heatwave metrics to ocean model resolution. *Geophysical Research Letters*, *46*, 14,604–14,612. https://doi.org/10.1029/2019GL084928

Received 12 AUG 2019
Accepted 3 DEC 2019
Accepted article online 9 DEC 2019
Published online 26 DEC 2019

Abstract Sustained extreme temperature events in the ocean, referred to as marine heatwaves (MHWs), generate substantial ecological, social, and economic impacts. Ocean models provide insights to the drivers, persistence, and dissipation of MHWs. However, the sensitivity of MHW metrics to ocean model resolution is unknown. Here, we analyze global MHW metrics in three configurations of a global ocean-sea ice model at coarse (1°), eddy-permitting (0.25°), and eddy-rich (0.1°) resolutions. We show that all configurations qualitatively represent broad-scale global patterns of MHWs. These simulated MHWs are, however, weaker, longer-lasting, and less frequent than in observations. The 0.1° configuration, despite local biases, performs best both globally and regionally. Based on these results, model projections of future MHW metrics using coarse-resolution models are expected to be biased toward weaker and less frequent MHWs, when compared with results using an eddy-rich model.

Plain Language Summary Marine heatwaves (MHWs) are persistent extreme temperatures in the ocean. They have a negative impact on marine life, fisheries, and tourism, and are becoming more frequent and more intense. One way to understand how MHWs form, intensify, and decay is by analyzing results from computer simulations of the ocean. However, these simulations are a simplification of reality, and depending on how they are designed they represent different aspects of the ocean circulation. It is still unknown how much the resolution of an ocean simulation matters when representing MHWs. In this work, we compare the performance of three ocean simulations—with low, medium, and high resolutions—when representing MHWs. We find that, regardless of their resolution, all simulations have weaker, longer, and less-frequent MHWs, when compared with the real world. Despite these differences, we find that simulations with medium and high-resolutions realistically represent global spatial patterns of MHWs. However, the ocean simulation with high resolution is preferable when studying regional patterns of MHWs. These results show how simulated MHWs differ from the real world, helping us to improve ocean simulations to be more realistic. In addition, we now better understand how computer simulations of future oceans, under climate change conditions, represent these extreme events.

1. Introduction

The ocean is warming, both near the surface and in the abyss (Cheng et al., 2019; Durack et al., 2018; Purkey & Johnson, 2010). In addition to this underlying warming, temperature extremes are becoming more frequent and more intense (Frölicher et al., 2018; Oliver et al., 2018; Scannell et al., 2016), and are projected to continue to intensify in response to increasing greenhouse forcing (Darmaraki et al., 2019; Frölicher et al., 2018). The occurrence of sustained temperature extremes leads to marine heatwave (MHW) conditions in the ocean (Hobday et al., 2016). MHW conditions are caused by local processes that directly affect ocean temperature, such as extreme air-sea heat fluxes and changes in the ocean circulation (Behrens et al., 2019; Holbrook et al., 2019; Salinger et al., 2019), which may ultimately be caused by large-scale climate forcing via teleconnection processes (Holbrook et al., 2019).

Discrete MHW events have been linked to higher substantial ecological, social, and economical impacts than to a long-term ocean warming (Collins et al., 2019; Smale et al., 2019). These impacts include permanent changes in the structure and functioning of ecosystems (Garrabou et al., 2009; Wernberg et al., 2013, 2016), mass mortality of economically relevant species, and decrease in catch or closure in fisheries (Cavole et al., 2016; Mills et al., 2013; Oliver et al., 2017).

©2019. American Geophysical Union. All Rights Reserved.

As the impacts of MHWs will likely continue in the future (Darmaraki et al., 2019; Frölicher et al., 2018), it is important to improve our knowledge of both the local and remote processes that lead to MHW conditions in the ocean and to, ultimately, predict these conditions. Three-dimensional ocean models are a valuable tool to explore key mechanisms that lead to MHW conditions, aiding our overall understanding of these extremes (e.g., Behrens et al., 2019; Oliver et al., 2017; Perkins-Kirkpatrick et al., 2018).

Studies on global (Frölicher et al., 2018) and regional (Darmaraki et al., 2019) MHW mean properties show that both coarse- and high-resolution coupled ocean-atmosphere models simulate weaker and longer MHWs, when compared with observations. However, in regional studies, high-resolution models have been shown to realistically simulate both the magnitude and spatial structure of specific MHW events (Benthuysen et al., 2014; Chen et al., 2014; Oliver et al., 2017). These results suggest that there is still ambiguity in the ability of high-resolution models to simulate MHWs, motivating a focused assessment of ocean model biases. Quantifying model biases provides more confidence when investigating model outputs to understand MHW drivers. This knowledge becomes especially important when interpreting characteristics of MHWs under future climate scenarios, for which no model evaluation can be made.

It is expected that ocean models with different resolutions simulate temperature extremes differently. For example, models of different spatial resolutions have different parameterizations and limitations and, therefore, resolve different local and remote processes that lead to MHW conditions. As models have increasingly higher spatial resolutions, improved representation of MHW characteristics is expected. However, whether this improvement is obtained, or if new model biases emerge in high-resolution configurations, remains unchecked. More importantly, because different models resolve different features, a comparison of models with different spatial resolutions would help to identify processes that lead to MHW conditions in each configuration. Understanding differences in MHW events in models of differing resolution not only helps to determine the appropriate spatial resolution of models for MHW studies but also builds the process-based understanding of MHWs.

Here, we investigate the ability of a global ocean-sea ice model with different configurations to simulate MHWs. Specifically, we compare the duration, intensity, and frequency of MHW events as simulated in a coarse (1°), an eddy-permitting (0.25°), and an eddy-rich (0.1°) configuration of a global ocean-sea ice model, as well as in an observation-based product. Our goal is to evaluate the sensitivity of the simulated MHW metrics to ocean model resolution.

2. Data and Methods

2.1. Ocean Model

The model used in this study is the Australian Community Climate and Earth System Simulator Ocean Model version 2 (ACCESS-OM2, Kiss et al., 2019), comprising three configurations with different horizontal grid spacings, nominally, 1°, 0.25°, and 0.1° (hereafter ACCESS-OM2, ACCESS-OM2-025, and ACCESS-OM2-01, respectively). To facilitate comparison between the different model configurations, the variations in resolution are available with identical code, forcing and, as far as possible, parameters.

ACCESS-OM2 is a coupled ocean and sea ice model, comprising the Modular Ocean Model version 5.1 (Griffies, 2012) and the Los Alamos Sea Ice Model CICE version 5.1.2 (Hunke et al., 2015). The model is forced by prescribed atmosphere conditions from the 55 year Japanese Reanalysis for driving oceans (JRA-55-do version 1.3, Tsujino et al., 2018). This product provides 3-hourly liquid and solid precipitation, sea level pressure, downward surface longwave and shortwave radiation, 10 m wind velocity components, 10 m specific humidity, and 10 m air temperature at roughly 0.5° resolution, and daily river flux at 0.25° resolution. In all three configurations, the model grid extends from the Antarctic ice shelf edge to the North Pole.

The initialization processes and spin-up in the three model configurations varies. ACCESS-OM2 and ACCESS-OM2-025 start at rest, and with temperature and salinity from a monthly climatology of the World Ocean Atlas 2013 v2 (WOCE; Locarnini et al., 2013; Zweng et al., 2013). These low-resolution configurations run for five 60 year (1958–2017) cycles of JRA-55-do.

The eddy-rich configuration, ACCESS-OM2-01, starts from a 40-year spin-up under repeated 1984–1985 year forcing, which in turn began from the same WOCE initial conditions as the coarser-resolution model configurations. Although this eddy-rich model has had less time to spin-up than the coarser models, the

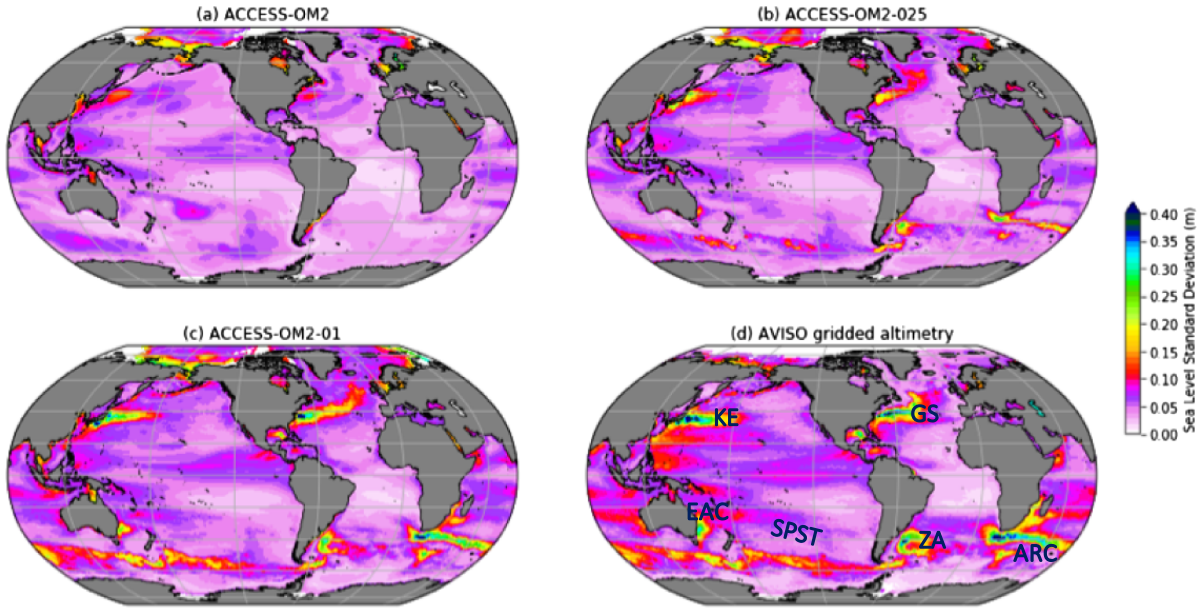

Figure 1. Maps of sea level standard deviation, in meters, for the years 1993–2017 in (a) the coarse-resolution model configuration (ACCESS-OM2), (b) the eddy-permitting model configuration (ACCESS-OM2-025), (c) the eddy-rich model configuration (ACCESS-OM2-01), and (d) Aviso's satellite altimetry product (adapted from Kiss et al., 2019). Labels in (d) indicate the Kuroshio Extension (KE), the Gulf Stream (GS), the East Australian Current (EAC), the South Pacific storm-track (SPST), Zapiola Anticyclone (ZA), and the Agulhas Return Current (ARC).

upper ocean is very close to equilibrium, with drifts in the surface temperature, surface salinity, and total kinetic energy comparable to those at the end of the longer runs at lower resolution (see Figure 3, in Kiss et al., 2019).

Known biases in the model include differences in the intensity and mean location of some western boundary currents (WBCs) relative to observations, and the representation of the mesoscale (Kiss et al., 2019). Here, we refer to model biases as the differences between models and observations. These biases are seen in maps of standard deviation of modeled sea level compared with satellite-sensed sea level from Aviso (Figure 1). The patterns of sea level variability in ACCESS-OM2-01 (Figure 1c) most closely resemble the patterns in observations (Figure 1d), but are not as high as the observed values. Examples of this lower modeled variability are seen in the East Australian Current, the Zapiola Anticyclone, the Agulhas Return Current, and the South Pacific storm track. In some regions, there are also differences in the mean location of strong modeled sea level variability compared with observations. An example is the North Atlantic, where the modeled Gulf Stream is displaced to the south and extends further east, compared with observations.

2.2. Observations

We compare the MHW metrics calculated from each simulation to MHW metrics calculated from an observation-based product. For this comparison, we use the National Oceanic and Atmospheric Administration sea surface temperature (SST) product, developed using optimum interpolation (NOAA-OI, Reynolds et al., 2007). This data set is a global, daily, high-resolution (0.25°) gridded product, built using Advanced Very High Resolution Radiometer infrared satellite data and in situ measurements. This product represents the temperature in the top 0.5 m of the ocean, achieved by regressing the satellite measurement of the ocean skin layer against quality-controlled buoy data. For comparison with the model runs, we analyze the NOAA-OI SST data between January 1985 and December 2017.

An Advanced Very High Resolution Radiometer-only data set such as NOAA-OI guarantees moderate homogeneity in time (Fiedler et al., 2019), but it does not include measures of SST under cloud coverage. Clouds remain the largest source of negative bias in the data, especially in the western boundary of the oceans, the tropics, and during winter months (Reynolds et al., 2007). In western boundary regions, however, slow-moving features are still well captured in the final gridded product (Reynolds et al., 2007). Other sources of bias are atmospheric aerosols, and instrument design and aging. Despite these biases, NOAA-OI has been widely used in MHW studies due to its temporal and spatial resolution, long record, and global

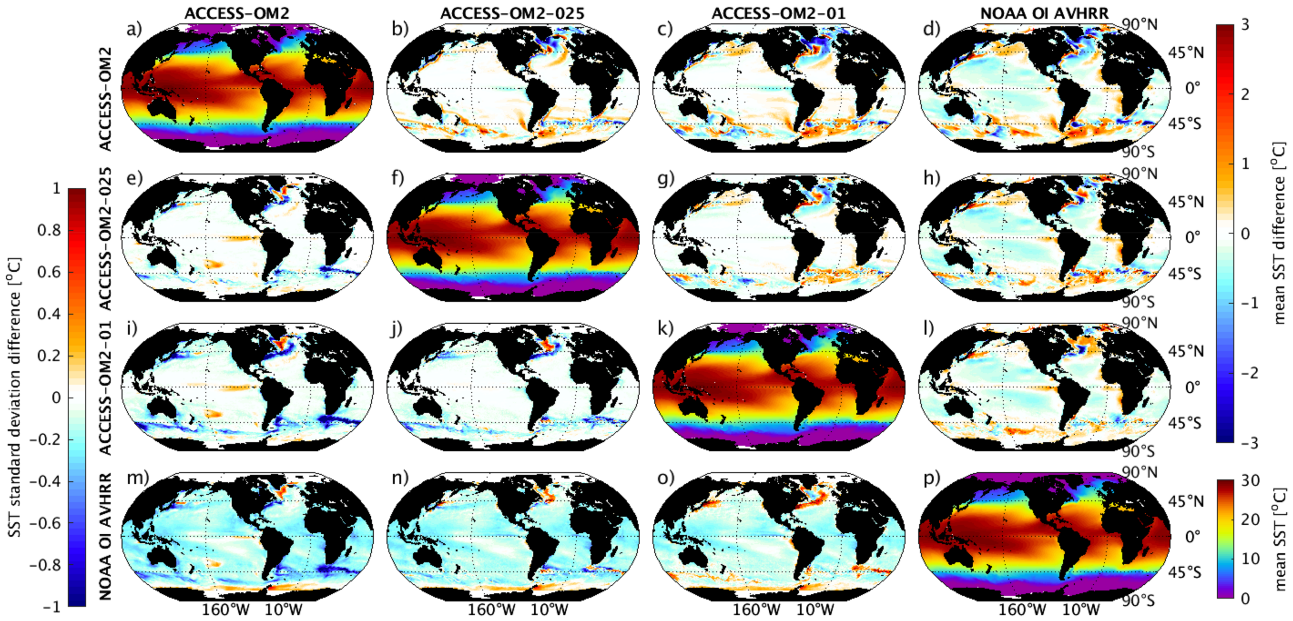

Figure 2. Comparisons between modeled and observed mean and standard deviation of deseasonalized SST for the years 1985–2017. The diagonal shows mean SST for the three runs of ACCESS-OM2 (a, f, and k) and for the NOAA-OI observation-based product (p). The maps above the diagonal show mean SST differences between the model runs and NOAA-OI (i.e., model-observations; d, h, l), and the model runs of different resolutions (i.e., lower resolution-higher resolution, b, c, g). The maps below the diagonal show SST standard deviation differences between the model runs and NOAA-OI (i.e., model-observations; m, n, o), and the model runs of different resolutions (i.e., lower resolution-higher resolution; e, i, j).

coverage (e.g., Frölicher & Laufkötter, 2018; Hobday et al., 2016; Holbrook et al., 2019; Manta et al., 2018; Oliver et al., 2017; Smale et al., 2019). The results relative to NOAA-OI presented here are comparable to previous MHW studies—because the same biases are present in those studies.

2.3. MHW Analysis

We identify MHWs in daily SST fields from the model runs and from the observation-based product following the definition proposed by Hobday et al. (2016). By following this definition, we aim to facilitate comparisons between our results and previous and future MHW studies. As in Hobday et al. (2016), a MHW is a period of at least 5 days where the ocean temperature is warmer than the 90th percentile above the climatological value for that location and time of the year.

We first regrid the three model configurations to the observation grid (i.e., 0.25°) by performing a first-order conservative remapping (Jones, 1999), then calculate SST mean, SST standard deviation, and MHW metrics. We choose to regrid the data before performing these calculations to eliminate the higher variance due to fine-scale features in ACCESS-OM2-01. This procedure emulates the gridding process of the observation-based product, which eliminates the fine-scale variations contained in the along-track sensed SST.

We calculate the climatology and the 90th percentile for each regridded model configuration and the observation-based product. Calculating the climatology and threshold for each model configuration removes biases in the mean temperature for each simulation. For the MHW analysis between 1985 and 2017 we use the period between January 1985 and December 2014 (i.e., 20 years) to construct the climatology, and retain the SST trend, following Hobday et al. (2016). Both the climatology and the 90th percentile, at each grid cell, are calculated using all data within an 11-day window centered on each day of the year, ensuring sufficient sample size for percentile estimation.

The MHW definition is not developed with ice-covered regions in mind, impacting the 90th percentile threshold calculations depending on ice-melt rate. In addition, the sea ice is able to create leads and fractures in the eddy-rich model (Kiss et al., 2019), but not in the coarser models, complicating a comparison in those regions. Therefore, we limit our analysis to regions without a seasonal ice-coverage (i.e., latitudes between 70°S and 70°N). The MHW metrics analyzed here are the MHW mean intensity (mean SST above

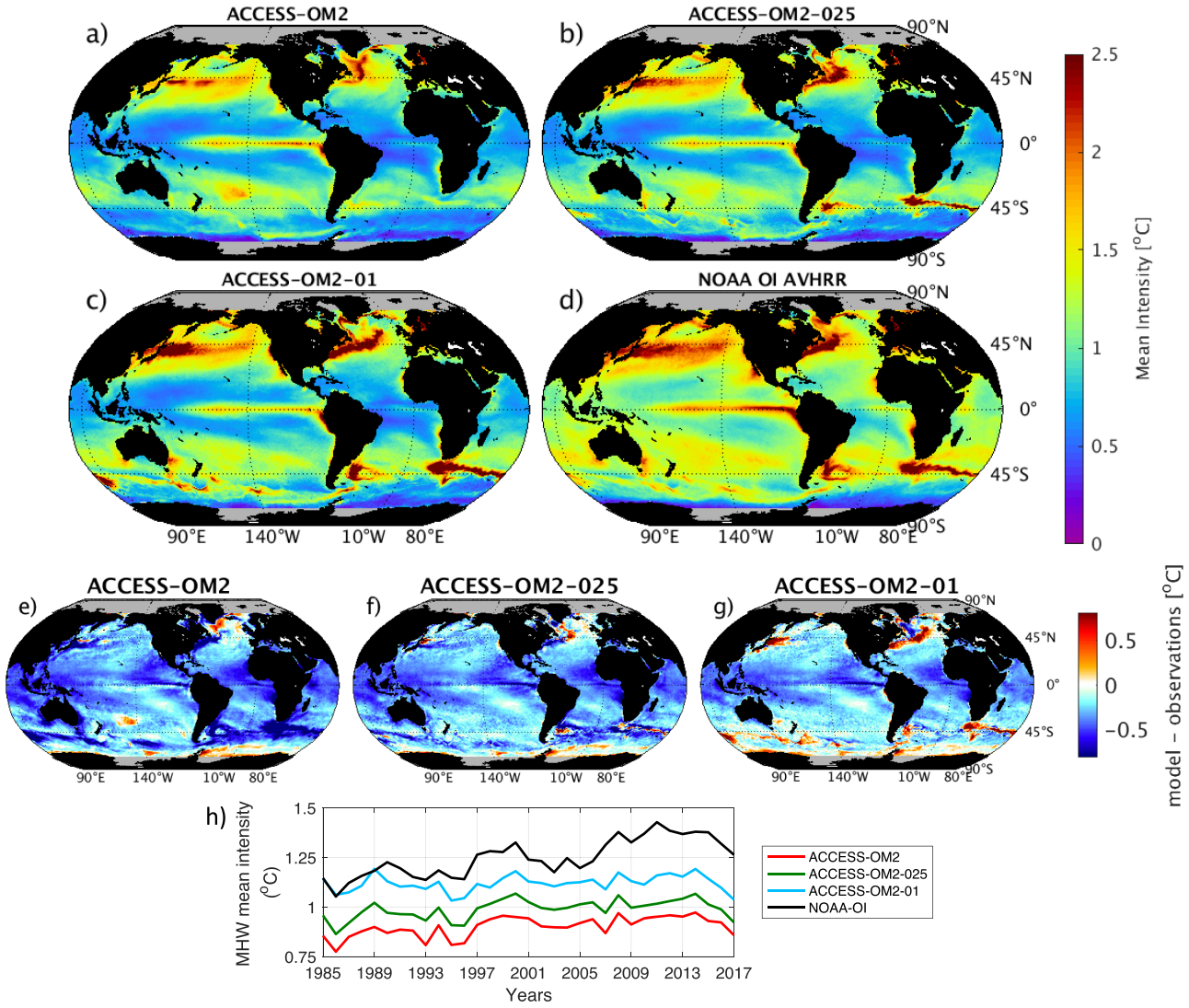

Figure 3. Maps of mean MHW intensity for the years 1985–2017 in (a) a coarse, (b) an eddy-permitting, and (c) an eddy-rich configuration of ACCESS-OM2, and (d) the NOAA-OI observation-based product; (e–g) mean MHW intensity bias (model-observations) for the three model configurations; (h) annual mean MHW intensity (70°S to 70°N) for each data set.

the climatology considering all days of a MHW event), MHW mean duration (number of sequential days where the SST exceeds the 90th percentile), and MHW mean frequency (number of MHW events per year).

3. Results

3.1. Comparison of SST

We start by analyzing how the model configurations compare with each other, and with observations, when simulating SST for the entire period (i.e., 1985–2017; Figure 2). The global patterns of mean SST in the model configurations and observations are comparable (Figure 2, diagonal), with exceptions in the center of the subtropical gyres (i.e., cold SST bias; Figures 2d, 2h, and 2l). Colder simulated SST might relate to thicker surface levels in the models (i.e., 2.3 and 1.1 m) compared with a thinner surface layer in NOAA-OI (i.e., representative of the top 0.5 m). In highly energetic regions, all model configurations simulate biases of up to 3 °C compared with NOAA-OI. As model resolution increases, these model biases are reduced. The improved performance of the eddy-rich configuration might be attributed to its explicit representation of oceanic processes, and to a shorter integration time, compared with the coarser configurations.

All model configurations underestimate SST variability in the tropics and overestimate SST variability in the subpolar regions compared with observations (Figures 2m–2o). Here, SST variability is calculated as the

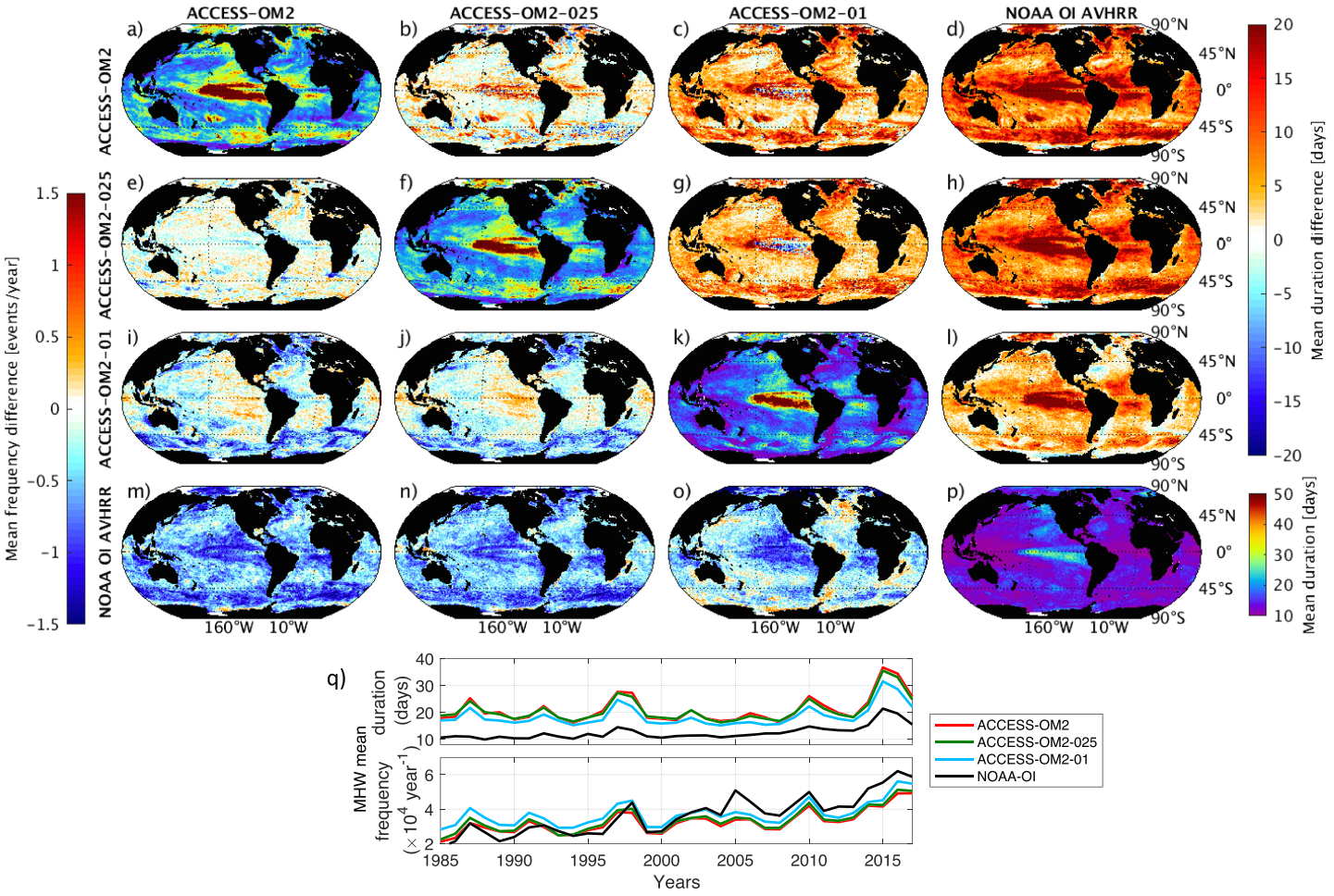

Figure 4. Comparisons between modeled and observed mean duration and frequency of MHWs for the years 1985–2017. The diagonal shows mean duration of MHWs for the three runs of ACCESS-OM2 (a, f, and k) and for the NOAA-OI observation-based product (p). The maps above the diagonal show differences in the mean duration of MHWs between the model runs and NOAA-OI (i.e., model-observations; d, h, l), and the model runs of different resolutions (i.e., lower resolution-higher resolution, b, c, g). The maps below the diagonal show differences in the mean frequency of MHWs between the model runs and NOAA-OI (i.e., model-observations; m, n, o), and the model runs of different resolutions (i.e. lower resolution-higher resolution; e, i, j). The time series (h) are the annual mean MHW duration (top) and frequency (bottom) between 70°S and 70°N, for each data set.

standard deviation of deseasonalized daily SST (i.e., we removed the climatology relative to each day of the year from the time series). The largest biases in SST variability in the coarse models relate to nonresolution of mesoscale features (Figures 2m and 2n). In the eddy-rich model (Figure 2o), the largest biases relate to an unrealistic representation of the mean ocean state (i.e., displaced ocean currents), as shown in Figure 1. There is a region of high variability in the South Pacific Ocean, to the east of New Zealand, only existent in ACCESS-OM2.

3.2. Comparison of MHW Metrics

The mean intensity of MHWs in the different model configurations is, overall, qualitatively similar to observations, but there are quantitative biases (Figure 3). The models simulate general patterns of intense MHWs in WBC regions, the tropics, and along the storm tracks in the South Pacific Ocean (i.e., from southern South America to northern Australia; O'Kane et al., 2014, Figures 3a–3d). Exceptions are highly energetic regions, such as the Zapiola Anticyclone and the Agulhas Return Current, where ACCESS-OM2 does not perform well. Patterns of MHW intensity bias in Figure 3 resemble patterns of SST variance bias (Figure 2), corroborating with the findings in Oliver et al. (2018).

Overall, the simulated MHWs are generally weaker, by up to 1 °C, in all model configurations (Figures 3e–3g). There is significant improvement in the mean intensity of simulated MHWs in the eddy-rich ACCESS-OM2-01, with biases reduced by 50% in the interior of the subtropical gyres (Figures 3e–3g). These

results show the importance of the mesoscale in driving temperature extremes in the ocean. Exceptions to the systematically weak modeled MHWs are intense MHWs to the east of New Zealand (160°W, 30°S; Figure 3e) in ACCESS-OM2, and in eddy-rich regions in ACCESS-OM2-01 (Figure 3g). In ACCESS-OM2-01, at the western boundaries, the biases in MHW intensity are mostly associated with deficiencies in the modeled WBCs, highlighted in section 2 (Figure 1).

Global annual means of MHW intensity show the impact of model resolution when simulating MHW metrics, with simulated values closer to observed values in ACCESS-OM2-01(Figure 3h). The MHWs identified in the NOAA-OI data set have a global positive trend of 0.0081 °C/year in their mean intensity. The simulated MHWs, however, do not follow this trend (with trends of 0.0031, 0.0025, and 0.0009 °C/year, for ACCESS-OM2, ACCESS-OM2-025, and ACCESS-OM2-01, respectively). These different trends between the models and observations are also seen in globally averaged SST (Figure 3 in Kiss et al., 2019). Despite these differences in global trends, simulated MHWs in all model resolutions follow sudden MHW intensity decreases after 1994, 2008, and 2014.

Globally, all models simulate longer and less frequent MHWs compared with observations (Figures 4d, 4h, 4l, 4m, 4n, and 4o). Even in the less-biased eddy-rich configuration, MHWs last for up to 25 days longer than in NOAA-OI. Long-lasting and less frequent simulated MHWs in the tropics can be explained by the maps of SST variability in Figure 2. In the tropics, the SST is more variable in observations than in the models. When SST varies at sufficiently high frequency, this variability can interrupt MHWs and thereby increase their number. A potential reason for longer-duration modeled MHWs is that the time series of SST are smoother in models compared with observations, due to their longer autocorrelation time (e.g., Cooper, 2017). Exceptions to these systematic biases in MHW duration and frequency are the WBCs in ACCESS-OM2-01. In this configuration, because the patterns of variability associated with WBCs are displaced (Figure 1), the simulated MHWs are also displaced. The slightly shorter, more frequent simulated MHWs compared with NOAA-OI seen in Figures 4l and 4o are a result of this displacement.

The impact of model resolution is not clearly seen in global annual means of MHW duration and frequency, with model runs performing similarly (Figure 4q). For MHW duration, ACCESS-OM2 has a ∼10% improvement on the representation of these MHW metrics (Figure 4q, top). This improvement is seen in the decrease in mean MHW duration in ACCESS-OM2-01, with values approaching, but still ∼7 days higher than, observations. All configurations simulate peaks of MHW mean duration seen in NOAA-OI (i.e., peaks in 1992, 1997, 2010, and 2015).

4. Discussion and Final Considerations

This study investigates the value of increasing model resolution for MHW studies. First, we show that the coarse model (i.e., 1° resolution) does not simulate the main MHW drivers in eddy-rich regions, leading to a lack of intense MHWs in WBCs. Nevertheless, global spatial patterns of MHW metrics resemble observed spatial patterns in quiescent regions of the ocean. Second, we show that the eddy-permitting model (i.e., 0.25° resolution) performs better than the coarser model, both quantitatively and qualitatively, in simulating MHWs globally. Therefore, an eddy-permitting model can be used, with caution, when considering the cost-benefit of analyzing a global ocean model in MHW studies. Third, we show that the eddy-rich model (i.e., 0.1° resolution) has the most realistic representation of MHWs characteristics, both globally and regionally. We conclude, therefore, that the resolution of the model analyzed in a MHW study should be dictated by the purpose and scale of the investigation.

The biases in MHW metrics shown here, in historical runs at different resolutions, should also be seen in projection runs of different resolutions. There is currently a suite of resolutions of global ocean model projection runs completed, including coarse (CMIP5; e.g., Frölicher et al., 2018), and eddy-rich (e.g., Zhang et al., 2017) simulations. In the near-future, some CMIP6 runs will have an eddy-permitting resolution (Eyring et al., 2016). Therefore, when analyzing MHW metrics in projection runs, the associated biases in MHW metrics related to model resolution must be kept in mind. Our results provide insights into the likely accuracy of projections of MHWs under climate change scenarios at different model resolutions.

In our analysis, MHWs are more persistent in models than in observations. This is also true for atmospheric heatwaves (Plavcová & Kyselý, 2016). Using a suite of atmospheric regional climate models, Plavcová and Kyselý (2016) attempt to mitigate the positive bias in heatwave duration. To achieve this, the authors increase

the period that defines an atmospheric heatwave from 3 to 5 days. Then, they apply this new definition to both the model and observations. Even with a longer temporal threshold, the modeled atmospheric heatwaves are still more persistent than the observed heatwaves. Here, we show biases of up to ±1 °C in the modeled SST variability in most of the ocean. Therefore, it is reasonable to expect that changing the temporal threshold in the MHW definition in both models and observations is unlikely to reduce the biases in MHW duration and frequency—as shown by Plavcová and Kyselý (2016).

The analysis performed here considers the SST to be the first vertical level of each model configuration. These levels are thinner in ACCESS-OM2-01 than in the coarser runs—posing a challenge to the comparisons shown here. One way to limit this challenge is to average the temperature of the top-three grid levels of ACCESS-OM2-01 (i.e., 0.5, 1.6, and 2.9 m thick), and then use this average for our analysis. For a quiescent region of the ocean (i.e., the Great Australian Bight, south of Australia), we find that this calculation does not reduce differences in MHW metrics between this configuration and the coarser configurations, only reducing the bias of ACCESS-OM2-01 by ~10%. Therefore, averaging the top surface levels of the high-resolution, eddy-rich model is insufficient to ease comparisons. Differences in level thickness also lead to differences in the influence of the wind stress on the ocean's heat uptake (Stewart & Hogg, 2019). This wind stress influence is not corrected when the top levels of ACCESS-OM2-01 are averaged, and this lack of correction might add more biases to the final result.

Regardless of their resolution, all ocean models have biases in MHW mean intensity, frequency, and duration. These biases are, overall, systematic and bias correction techniques could be applied to the data. However, determining how much bias is acceptable, and if a bias correction is possible, depends on the question being asked and on the nature of the MHW study (e.g., Maraun, 2016). Moreover, bias correction can become problematic, as it may not represent the true physics within the system, and misrepresent important feedbacks and processes in ocean and climate systems (Maraun, 2016). Our results indicate that a justifiable way to reduce bias in model representation of MHWs is by increasing the model resolution. High-resolution models require less parameterization but provide more explicit representation of key processes at the relevant scales, thereby reducing the call for large bias corrections.

The results in this paper indicate where the representation of MHWs in non-eddy-resolving models must be improved. We show that ACCESS-OM2 represents some patterns of MHW metrics, but not in important eddying regions, such as the Zapiola Anticyclone and the Agulhas Return Current. We also show that ACCESS-OM2-025 represents all the global MHW metrics, albeit with biases, compared with observations and with ACCESS-OM2-01. Hence, this study highlights the need to further develop model parameterizations for MHW studies in non-eddy-resolving models, such as those typically used for climate projections.

Acknowledgments
The authors thank the Consortium for Ocean-Sea Ice Modeling in Australia (COSIMA; www.cosima.org.au), funded by the Australian Research Council through its Linkage Program (LP160100073), for making the ACCESS-OM2 suite of models available in https://doi.org/10.5281/zenodo.2653246 (Hannah et al., 2019) and in this site (https://github.com/COSIMA/access-om2). All model components are open source. The model output for the simulations presented in this manuscript will be stored on the COSIMA data collection, available in this website (https://doi.org/10.4225/41/5a2dc8543105a). This research was undertaken with the assistance of resources from the National Computational Infrastructure (NCI), which is supported by the Australian Government. Sea level products were processed by SSALTO/DUACS and distributed by AVISO+ with support from CNES. We acknowledge support from the ARC Centre of Excellence for Climate Extremes (CE170100023). We thank H. Hayashida for discussions about this work. Some of the code used to perform this analysis was written and made publicly available by Z. Zhao and M. Marin (Zhao & Marin, 2019).

References

Behrens, E., Fernandez, D., & Sutton, P. (2019). Meridional oceanic heat transport influences marine heatwaves in the Tasman Sea on interannual to decadal timescales. *Frontiers in Marine Science*, *6*, 228.

Benthuysen, J., Feng, M., & Zhong, L. (2014). Spatial patterns of warming off Western Australia during the 2011 Ningaloo Nino: Quantifying impacts of remote and local forcing. *Continental Shelf Research*, *91*, 232–246.

Cavole, L., Demko, A., Diner, R., Giddings, A., Koester, I., Pagniello, C., et al. (2016). Biological impacts of the 2013–2015 warm-water anomaly in the northeast pacific: Winners, losers, and the future. *Oceanography*, *29*(2). https:doi.org/10.5670/oceanog.2016.32

Chen, K., Gawarkiewicz, G. G., Lentz, S. J., & Bane, J. M. (2014). Diagnosing the warming of the Northeastern U.S. Coastal Ocean in 2012: A linkage between the atmospheric jet stream variability and ocean response. *Journal of Geophysical Research: Oceans*, *119*, 218–227. https:doi.org/10.1002/2013JC009393

Cheng, L., Abraham, J., Hausfather, Z., & Trenberth, K. E. (2019). How fast are the oceans warming? *Science (80)*, *363*(6423), 128–129. https://doi.org/10.1126/science.aav7619

Collins, M., Sutherland, M., Bouwer, L., Cheong, S. M., Frolicher, T., DesCombes, H. J., et al. (2019). Extremes, abrupt changes and managing risks. IPCC Spec. Rep. Ocean Cryosph. a Chang. Clim. In press, Chapter 6.

Cooper, F. C. (2017). Optimisation of an idealised primitive equation ocean model using stochastic parameterization. *Ocean Modelling*, *113*, 187–200.

Darmaraki, S., Somot, S., Sevault, F., Nabat, P., Cabos, N., William, D., et al. (2019). Future evolution of Marine Heatwaves in the Mediterranean Sea. *Climate Dynamics*, *5*(3), 1–2. https://doi.org/10.1007/s00382-019-04661-z

Durack, P., Gleckler, P., Purkey, S., Johnson, G., Lyman, J., & Boywe, T. (2018). Ocean warming: From the surface to the deep in observations and models. *Oceanography*, *31*(2), 41–51. https://doi.org/10.5670/oceanog.2018.227

Eyring, V., Bony, S., Meehl, G. A., Senior, C. A., Stevens, B., Stouffer, R. J., & Taylor, K. E. (2016). Overview of the Coupled Model Intercomparison Project Phase 6 (CMIP6) experimental design and organization. *Geoscientific Model Development*, *9*(5), 1937–1958. https:/doi.org/10.5194/gmd-9-1937-2016

Fiedler, E. K., McLaren, A., Banzon, V., Brasnett, B., Ishizaki, S., Kennedy, J., & Donlon, C. (2019). Intercomparison of long-term sea surface temperature analyses using the GHRSST Multi-Product Ensemble (GMPE) system. *Remote Sensing of Environment*, *222*, 18–33. https://doi.org/10.1016/j.rse.2018.12.015

Frölicher, T. L., Fischer, E. M., & Gruber, N. (2018). Marine heatwaves under global warming. *Nature*, *560*(7718), 360–364. https://doi.org/10.1038/s41586-018-0383-9

Frölicher, T. L., & Laufkötter, C. (2018). Emerging risks from marine heat waves. *Nat Commun*, *9*(1), 2015–2018. https://doi.org/10.1038/s41467-018-03163-6

Garrabou, J., Coma, R., Bensoussan, N., Bally, M., Chevaldonne, P., Cigliano, M., et al. (2009). Mass mortality in Northwestern Mediterranean rocky benthic communities: Effects of the 2003 heat wave. *Global Change Biology*, *15*(5), 1090–1103. https://doi.org/10.1111/j.1365-2486.2008.01823.x

Griffies, S. M. (2012). Elements of the Modular Ocean Model (MOM) (2012 release with updates). 3(C); 632. http://mom-ocean.org/web/docs/project/MOM5_manual.pdf

Hannah, N., Ward, M. L., Fiedler, R., Heerdegen, A., Hogg, A. McC., & Kiss, A. E. (2019). The ACCESS-OM2 global ocean-sea ice coupled model. https://doi.org/10.5281/zenodo.2653246

Hobday, A. J., Alexander, L. V., Perkins, S. E., Smale, D. A., Straub, S. C., Oliver, E. C. J., et al. (2016). Progress in oceanography: A hierarchical approach to defining marine heatwaves. *Progress in Oceanography*, *141*, 227–238. https://doi.org/10.1016/j.pocean.2015.12.014

Holbrook, N., Scannell, H. A., Sen Gupta, A., Benthuysen, J., Feng, M., Oliver, E. C., et al. (2019). A global assessment of marine heatwaves and their drivers. *Nature Communications*, *10*(2624), 1–13. https://doi.org/10.1038/s41467-019-10206-z

Hunke, E. C., Lipscomb, W. H., Turner, A. K., Jeffery, N., & Elliot, S. (2015). CICE: The Los Alamos sea ice model documentation and software user's manual version 5.1. (Tech. Rep.)

Jones, P. W. (1999). First-and second-order conservative remapping schemes for grids in spherical coordinates. *Monthly Weather Review*, *127*(9), 2204–2210.

Kiss, A. E., Hogg, A. M., Hannah, N., Boeira Dias, F., Brassington, G. B., Chamberlain, M. A., et al. (2019). ACCESS-OM2 v1.0: A global ocean-sea ice model at three resolutions. *Geoscientific Model Development Discussions*, *2019*. https://doi.org/10.5194/gmd-2019-106

Locarnini, R. A., Mishonov, A. V., Antonov, J. I., Boyer, T. P., Garcia, H. E., Baranova, O. K., et al. (2013). World ocean atlas 2013 volume 1: Temperature. NOAA Atlas NESDIS 73.

Manta, G., de Mello, S., Trinchin, R., Badagian, J., & Barreiro, M. (2018). The 2017 record marine heatwave in the Southwestern Atlantic Shelf. *Geophysical Research Letters*, *45*, 12–449. https://doi.org/10.1029/2018GL081070

Maraun, D. (2016). Bias correcting climate change simulations—A critical review. *Current Climate Change Reports*, *2*(4), 211–220. https://doi.org/10.1007/s40641-016-0050-x

Mills, K. E., Pershing, A. J., Brown, C. J., Chen, Y., Chiang, F. S., Holland, D. S., et al. (2013). Fisheries management in a changing climate. *Oceanography*, *26*(2), 191–195.

O'Kane, T. J., Matear, R. J., Chamberlain, M. A., Oliver, E. C. J., & Holbrook, N. J. (2014). Storm tracks in the Southern Hemisphere subtropical oceans. *Journal of Geophysical Research: Oceans*, *119*, 6078–6100. https://doi.org/10.1002/2014JC009990

Oliver, E. C., Benthuysen, J. A., Bindoff, N. L., Hobday, A. J., Holbrook, N. J., Mundy, C. N., & Perkins-Kirkpatrick, S. E. (2017). The unprecedented 2015/16 Tasman Sea marine heatwave. *Nature Communications*, *8*, 1–12. https://doi.org/10.1038/ncomms16101

Oliver, E. C. J., Donat, M. G., Burrows, M. T., Moore, P. J., Smale, D. A., Alexander, L. V., et al. (2018). Longer and more frequent marine heatwaves over the past century. *Nature Communications*, *9*(1), 1324. https://doi.org/10.1038/s41467-018-03732-9

Perkins-Kirkpatrick, S. E., King, A., Cougnon, E., Grose, M., Oliver, E., Holbrook, N., et al. (2018). The role of natural variability and anthropogenic climate change in the 2017/18 Tasman Sea marine heatwave. *Bulletin of the American Meteorological Society*, *100*(1), 1–6. https://doi.org/10.1175/BAMS-D-18-0116.1

Plavcová, E., & Kyselý, J. (2016). Overly persistent circulation in climate models contributes to overestimated frequency and duration of heat waves and cold spells. *Climate Dynamics*, *46*(9-10), 2805–2820. https://doi.org/10.1007/s00382-015-2733-8

Purkey, S. G., & Johnson, G. C. (2010). Warming of global abyssal and deep Southern Ocean waters between the 1990s and 2000s: Contributions to global heat and sea level rise budgets. *Journal of Climate*, *23*(23), 6336–6351. https://doi.org/10.1175/2010JCLI3682.1

Reynolds, R. W., Smith, T. M., Liu, C., Chelton, D. B., Casey, K. S., & Schlax, M. G. (2007). Daily high-resolution-blended analyses for sea surface temperature. *Journal of Climate*, *20*(22), 5473–5496. https://doi.org/10.1175/2007JCLI1824.1

Salinger, J., Renwick, J., Behrens, E., Mullan, B., Diamond, H. J., Sirguey, P., et al. (2019). The unprecedented coupled ocean-atmosphere summer heatwave in the New Zealand region 2017/18: Drivers, mechanisms and impacts. *Environmental Research Letters*, *14*, 044023. https://doi.org/10.1088/1748-9326/ab012a

Scannell, H. A., Pershing, A. J., Alexander, M. A., Thomas, A. C., & Mills, K. E. (2016). Frequency of marine heatwaves in the North Atlantic and North Pacific since 1950. *Geophysical Research Letters*, *43*, 2069–2076. https://doi.org/10.1002/2015GL067308

Smale, D. A., Wernberg, T., Oliver, E. C. J., Thomsen, M., Harvey, B. P., Straub, S. C., et al. (2019). Marine heatwaves threaten global biodiversity and the provision of ecosystem services. *Nature Climate Change*, *9*, 306. https://doi.org/10.1038/s41558-019-0412-1

Stewart, K. D., & Hogg, A. M. (2019). Southern Ocean heat and momentum uptake. Accepted subject to minor revisions.

Tsujino, H., Urakawa, S., Nakano, H., Small, R. J., Kim, W. M., Danabasoglu, G., et al. (2018). JRA-55 based surface dataset for driving ocean-sea ice models (JRA55-do). *Ocean Modelling*, *130*, 79–139. https://doi.org/10.1016/j.ocemod.2018.07.002

Wernberg, T., Bennett, S., Babcock, R. C., de Bettignies, T., Cure, K., & Depczynski, M. (2016). Climate-driven regime shift of a temperate marine ecosystem. *Science (80-.)*, *353*(6295), 169–172. https://doi.org/10.1126/science.aad8745

Wernberg, T., Smale, D., Tuya, F., Thomsen, M. S., Langlois, T. J., De Bettignies, T., et al. (2013). An extreme climatic event alters marine ecosystem structure in a global biodiversity hotspot. *Nature Climate Change*, *3*(1), 78–82. https://doi.org/10.1038/nclimate1627

Zhang, X., Church, J. A., Monselesan, D., & McInnes, K. L. (2017). Sea level projections for the Australian region in the 21st century. *Geophysical Research Letters*, *44*, 8481–8491. https://doi.org/10.1002/2017GL074176

Zhao, Z., & Marin, M. (2019). A MATLAB toolbox to detect and analyze marine heatwaves. *Journal of Open Source Software*, *4*(33), 1124. https://doi.org/10.21105/joss.01124

Zweng, M., Reagan, J., Antonov, J., Locarnini, R., & Mishonov, A. (2013). World ocean atlas 2013, volume 2: Salinity. NOAA Atlas NESDIS 74.